PROCEEDINGS OF SCIENCE

A novel approach to $\tau \to \ell$ + invisible

Diego Guadagnoli[a,*]

[a] *LAPTh, Université Savoie Mont-Blanc et CNRS, 74941 Annecy, France*

E-mail: diego.guadagnoli@lapth.cnrs.fr

I discuss a novel approach to collider searches of $\tau \to \ell$ + invisible, where the invisible could be an axion-like particle or even a hidden photon. This talk is based on work in collaboration with Chan Beom Park and Francesco Tenchini.

Corfu Summer Institute 2021 "School and Workshops on Elementary Particle Physics and Gravity"
29 August - 9 October 2021
Corfu, Greece

*Speaker

https://pos.sissa.it/

PoS(CORFU2021)023

1. Context and Motivation

In recent years, there has been renewed interest in new light particles beyond the SM matter content. This is due to a concurrence of theoretical, phenomenological and experimental reasons. Such particles allow to elegantly address conceptual and also observational problems, see e.g. [1]. Their mass may be as large as 1 GeV, depending on the couplings structure. New scalars in the MeV-GeV mass range whose couplings to SM matter have a larger-than-weak strength are fully compatible with all measurements on stable matter [2]. In fact the strongest constraints, from astrophysical data, apply to 1^{st}-generation matter only. Finally, there is no intrinsic reason ruling that these particle should couple universally across generations, or in a flavour-diagonal way [3]. All these considerations make meson or τ decays at colliders very suited—also because of the large statistics and accuracy now attainable—to test new physics with the above properties.

Searches at colliders can be performed under the minimal assumption that the new particle leaves the detector volume undetected. One prototype search is then $\tau \to \ell + \phi$, where ℓ denotes a light lepton and ϕ an axion-like particle (ALP) [4]. The state-of-the-art dates back to Refs. [5, 6], and an new search is in progress at Belle II [7]. A crucial advantage of these facilities is that the total missing energy of the system is accurately known. For both signal and backgrounds, however, the presence of undetected particles prevents the reconstruction of the separate momenta of the pair-produced τs. In order to separate the signal, the reference strategy has been to try estimate the signal-τ momentum using the visible momenta on the tag side. E.g., in the method used by ARGUS [6] one considers $\tau \to 3\pi\nu$, and the signal-τ momentum may then be estimated as $\widehat{\boldsymbol{p}}_\tau \approx -\sum_i^{\text{tag}} \widehat{\boldsymbol{p}}_{\pi_i}$, $E_\tau \approx \sqrt{s}/2$ [6], where a hat denotes a unit vector. More generally, one may exploit the 'thrust axis' [8, 9] of the event, and approximate the signal-τ momentum [7] as

$$p_\tau = \frac{\sqrt{s}}{2}\left(1,\, \widehat{\boldsymbol{n}}\,\sqrt{1-4m_\tau^2/s}\right) . \tag{1}$$

This represents the current state-of-the-art method.

2. Our Method: Basics

Our method also aims at reconstructing the two τ's separate boosts. However, our approach is radically different from the state-of-the-art, in that we exploit the applicability of a different set of variables, never considered in this context, and that have a 'natural', built-in way of estimating the separate boosts that we aim at. In more detail, our approach is based on the following observations: *(i)* both signal and background decays consist of a pairwise decay topology, with visible final states on either branch, plus either the elusive ϕ (signal), or neutrinos (backgrounds). Such topology lends itself to the use of variables such as the 'stransverse mass' M_{T2} [10, 11] and its Lorentz-invariant generalisations [12]; *(ii)* denoting these variables collectively as M_2, we note that their algorithm (a minimisation in the invisible 3-momentum on either of the two decay chains) produces as outcome the so-called *M_2-Assisted On-Shell*, or 'MAOS', invisible momentum [13, 14]. The latter has a distribution centered around the *true* invisible 3-momentum, and thereby provides a 'built-in' estimator of the concerned invisible 3-momentum. This, plus the measured constraint on the total missing momentum, addresses the underlying challenge of the search; *(iii)* our approach is expected

to have little correlation with the state-of-the-art method, because the latter is based on variables built out of visible momenta only. Hence the two approaches may be profitably combined. We will show that this is indeed the case, and the combination provides a substantially higher performance than the case where the different variables discussed are used individually.

For the sake of definiteness, and also in order to have a benchmark to compare against, we apply our idea to $\tau \to \ell + \phi$, specializing ℓ to the electron in the numerics for consistency with the analysis in [7]. The search is thus for

$$e^+e^- \to \tau(\to \ell\phi)\ \tau(\to 3\pi\nu)\,, \tag{2}$$

where charge specifications are omitted on the r.h.s., and the ϕ is assumed to escape undetected. We henceforth refer to this channel as '1×3', with dominant irreducible background

$$e^+e^- \to \tau(\to \ell\nu\bar{\nu})\ \tau(\to 3\pi\nu)\,. \tag{3}$$

We will also consider the '1×1' channel $\tau(\to \ell\nu\bar{\nu})$, for which the ARGUS/thrust method is not applicable. Its irreducible background is $\tau(\to \ell\nu\bar{\nu})\tau(\to \ell\nu\bar{\nu})$.

The above decay topology is suitable for applying $M_{\rm T2}$ and its generalizations. Such variables have never been considered in the context of decays of pair-produced mesons or leptons. The $M_{\rm T2}$ variable is defined as [10, 11] i.e.

$$\begin{aligned} M_{\rm T2} =& \min_{\boldsymbol{k}_{1\rm T},\boldsymbol{k}_{2\rm T}}\Big[\max\Big\{M_{\rm T}(\boldsymbol{p}_{1\rm T},\,\boldsymbol{k}_{1\rm T}),\,M_{\rm T}(\boldsymbol{p}_{2\rm T},\,\boldsymbol{k}_{2\rm T})\Big\}\Big] \\ & \text{subject to } \boldsymbol{k}_{1\rm T}+\boldsymbol{k}_{2\rm T}=\boldsymbol{P}^{\rm miss}_{\rm T}, \end{aligned} \tag{4}$$

where "T" denotes the projection onto the plane transverse to the beam direction. Since our application is in the context of a lepton collider, whose initial-state kinematics is known, we will employ the fully Lorentz-invariant extension of $M_{\rm T2}$, known as M_2 [12] (see also [15, 16]). M_2 can actually be constructed in many ways, according to the kinematic constraints that are enforced in the minimisation. We focus on the following definition

$$\begin{aligned} M_2 =& \min_{\boldsymbol{k}_1,\boldsymbol{k}_2}\Big[\max\Big\{M(p_1,\,k_1),\,M(p_2,\,k_2)\Big\}\Big] \\ & \text{subject to } \begin{cases} \boldsymbol{k}_1+\boldsymbol{k}_2=\boldsymbol{P}^{\rm miss}, \\ (p_1+p_2+k_1+k_2)^2=s, \end{cases} \end{aligned} \tag{5}$$

with s the squared collision energy, and $p_i(k_i)$ the visible- (invisible-)system total momenta on the decay branch $i = 1, 2$.

One first property of the 'MAOS' momenta $\boldsymbol{k}^{\rm maos}_{1,2}$ that minimize eq. (5) is their usability as estimators of the *true* momenta $\boldsymbol{k}_{1,2}$ [13, 14]. In fact, M_2-based MAOS momenta [16, 17] are distributed symmetrically around the true momenta, and peak at the respective true values. Besides, M_2-based MAOS momenta are more efficient than the $M_{\rm T2}$-based counterparts [17], for various reasons detailed in Ref. [18].

3. Derived Variables

The $\boldsymbol{k}^{\rm maos}_{1,2}$ momenta can be used to construct any variable for signal-background discrimination that would require knowledge of the invisible momenta. We summarize here two examples of such

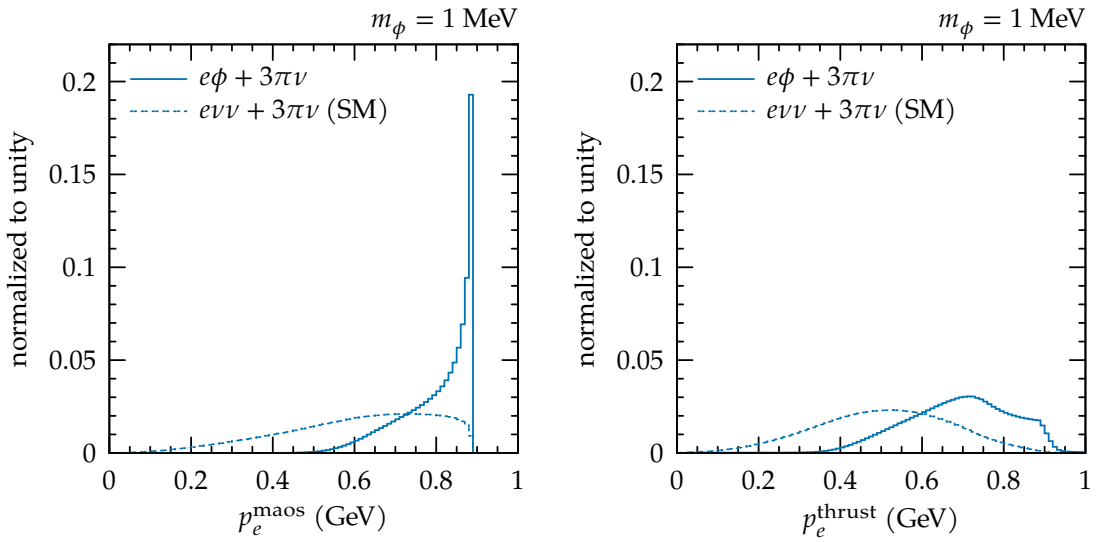

Figure 1: Distribution for $p_e^{\rm maos} \equiv |\boldsymbol{p}_e|^{\rm maos}_{\tau\text{-RF}}$ and for the same variable, calculated through the thrust. We consider the 1×3 channel and $m_\phi = 1$ MeV. Figure taken from Ref. [18].

variables. A first one is $|\boldsymbol{p}_\ell^{\tau\text{-RF}}|$ in the 1×3 channel. It is clear that, in the τ rest frame (RF), this quantity is the same as the signal-side invisible momentum. One can compare the boost estimated through the MAOS vs. thrust methods. Such comparison is shown in fig. 1 for the 1×3 channel and for $m_\phi = 1$ MeV, representative of the small-mass case. A second example is the ratio

$$\xi_k \equiv \frac{\min\{|\boldsymbol{k}_1|,\, |\boldsymbol{k}_2|\}}{\max\{|\boldsymbol{k}_1|,\, |\boldsymbol{k}_2|\}} \in [0,1]\,, \tag{6}$$

the corresponding ratio calculated with $\boldsymbol{k}_{1,2}^{\rm maos}$ being denoted with $\xi_k^{\rm maos}$. This quantity is reminiscent of the $R_{p_{\rm T}}$ ratio of Ref. [19]. However, there are two important differences: *(i)* $R_{p_{\rm T}}$ is constructed with the visible momenta, while ξ_k uses the separate invisible momenta on the two decay branches – which is precisely what MAOS provides; *(ii)* $R_{p_{\rm T}}$ is a 'max-over-min' ratio, taking values on the (non-compact) domain $[1, \infty]$. On the other hand, ξ_k spans the *compact* domain $[0, 1]$. The latter has the crucial advantage of enhancing the shape difference between signal and background, i.e. of not diluting it over a long distribution tail (which would be the case for a non-compact domain). The ξ_k distribution is displayed in fig. 2 (first panel), again for $m_\phi = 1$ MeV. We remark that $\xi_{k,p}$ may be defined in the lab or CMS frames. We observe that the slope differences are more pronounced in the CMS-frame definition. The ξ_k distribution may be compared with the ξ_p, $R_{k_{\rm T}}$ and $R_{p_{\rm T}}$ ones, shown in the remaining panels of fig. 2.

It is worth emphasizing the underlying rationale of eq. (6): this ratio should be closer to unity for more symmetric decay chains, e.g. the 1×1-channel background (4th entry in the legend). For the same reason, we also expect the ξ_k 'slope' to decrease as the number of invisibles decreases. Therefore, ξ_k is one example of 'invisible-savvy' variable, whose distribution is namely sensitive to the number of invisibles in the two decay branches.

One can further construct additional variables that do not require MAOS momenta, i.e. that can be computed from the visible momenta only. As such, these variables are expected to display a

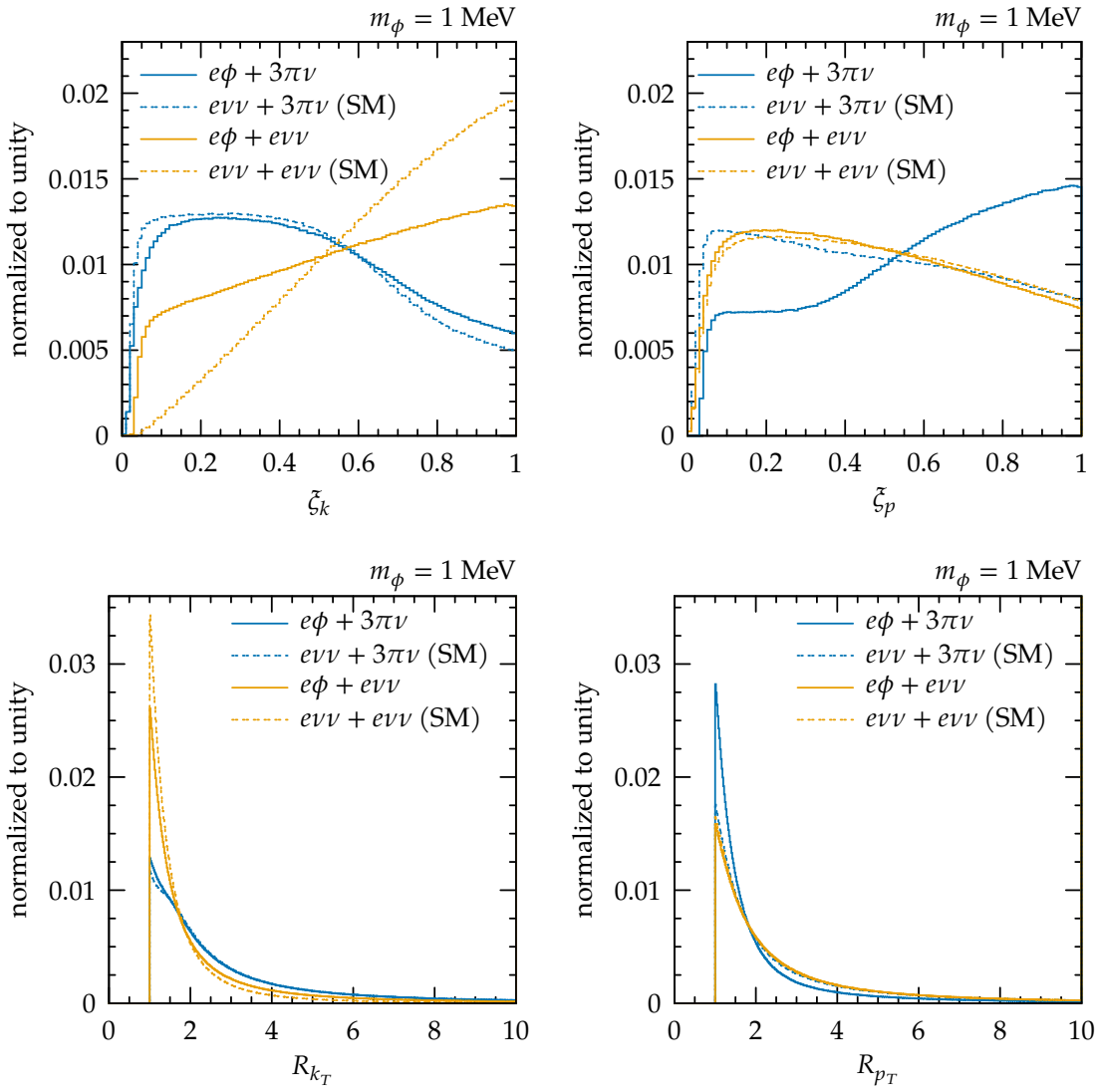

Figure 2: Distributions of the ratio variables $\xi_{k,p}$, R_{k_T,p_T} discussed below eq. (6), for the case $m_\phi = 1$ MeV. Figure taken from Ref. [18].

small enough correlation with those discussed so far. Examples of these variables include the recoil mass [20, 21] $M^2_{\text{recoil}} = (P^{\text{CMS}} - p_1 - p_2)^2$, i.e. the invariant mass of the full invisible system, as well as the variable $E_{\text{miss}} \equiv |\boldsymbol{P}_{\text{miss}}|$. For more details, that we omit here for brevity's sake, we refer the reader to Ref. [18].

4. Results

Our results are based on $e^+e^- \to \tau^+\tau^-$ decays obtained with `MadGraph`; tag-side decays and backgrounds are modeled through `TauDecay` [22], and signal-side decays are populated as phase space through `ROOT`. For each process considered we generate about $1.5 \cdot 10^7$ events. We also

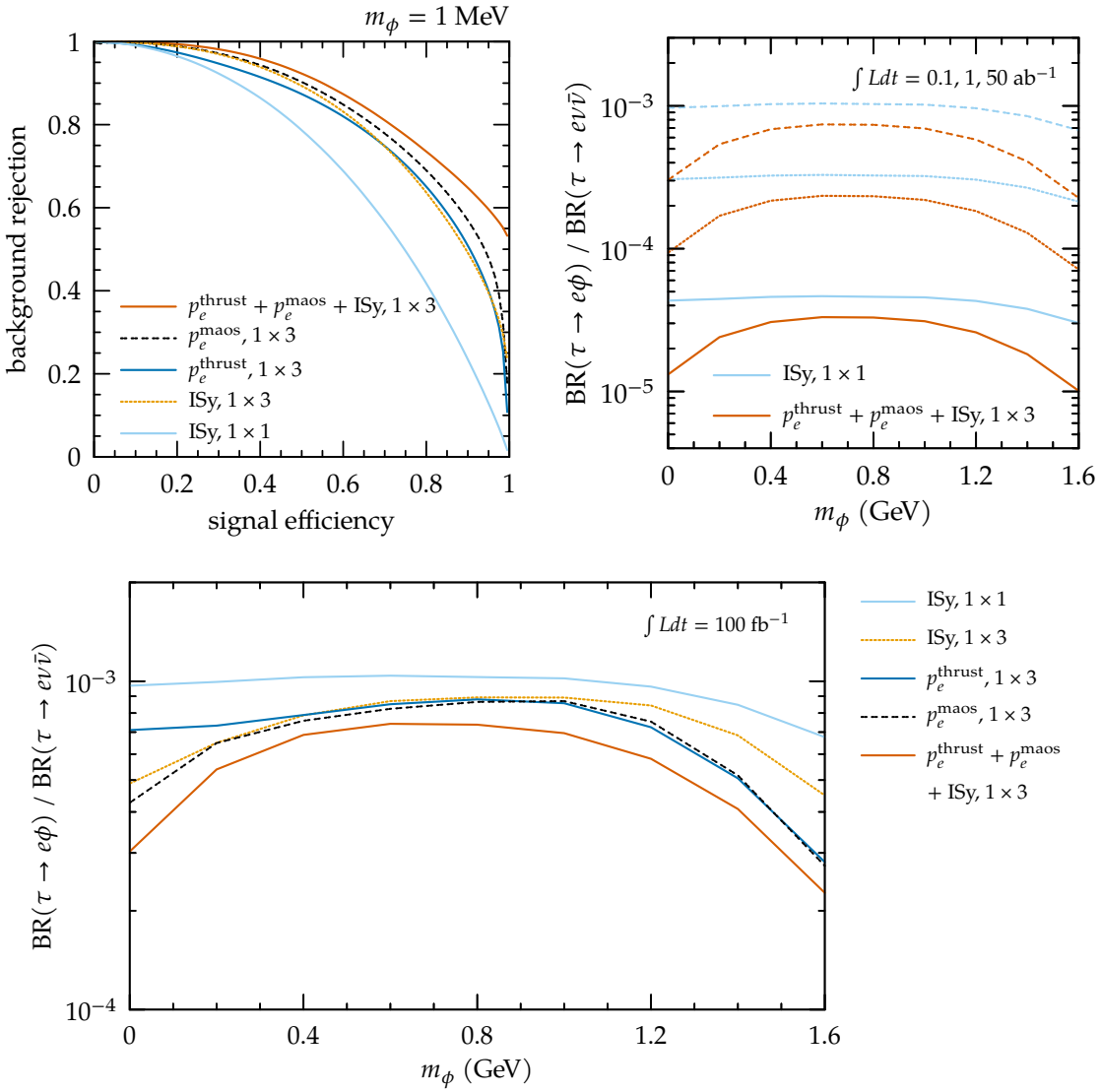

Figure 3: First panel: signal efficiency vs. background rejection in the different cases discussed in the text and in the case m_ϕ = 1 MeV. Second and third panels: 95% CL upper limits on the signal branching ratios normalized to the $\tau \to \ell\nu\nu$ one< as a function of the luminosity (second panel) or of the different cases discussed in the text (last panel). Figure panels taken from Ref. [18].

consider a number of cuts only for the sake of populating the phase space in a similar way as Ref. [7] and thereby make our event sample mimic this search as much as possible—whereas these cuts are otherwise unnecessary to optimize our variables. For more details see Ref. [18]. For the numerical analysis we use the public library `YAM2` [23] and the `TMVA` [24] class available in `ROOT`.

Let us now summarize our analysis. A first general point to be made is that M_2, $\xi_{k,p}$, $M_{\rm recoil}$ and $E_{\rm miss}$ are well-defined and calculable for both the 1×3 and 1×1 cases. Their distributions are sensitive to the number of invisibles in the decay and we thus collectively denote this set as 'invisible-savvy' variables. We construct with them the `ISy` classifier [18]. Note that $p_e^{\rm maos}$ is left

outside this classifier, in order again to allow for a closer comparison of our method with Ref. [7]. We inform our comparison by the following cases: *(a)* p_e^{thrust} alone, on 1×3 decays; *(b)* p_e^{maos} alone, on 1×3 decays; *(c)* `ISy` alone, on 1×3 decays; *(abc)* p_e^{thrust} + p_e^{maos} + `ISy` combined, on 1×3 decays; *(d)* `ISy`, on 1×1 decays. Case *(a)* serves as validation of our overall setup, because we fully reproduce the results in Ref. [7] in spite of our different MonteCarlo, analysis, and even of our completely different approach to translating the obtained S/B into branching-fraction limits (see Ref. [18]); the comparison across the cases *(a)*, *(b)*, *(c)* and *(abc)* serves to gauge the improvement achievable in the 1×3 channel alone; cases *(c)* vs. *(d)* provides a first test the relative performance of the 1×3 vs. 1×1 channels, keeping in mind that such test has many subtleties (again, see Ref. [18] for more details, including on why we refrained from discussing a possible *(abcd)* case).

The mentioned comparisons are shown in the plane of signal efficiency vs. background rejection in fig. 3 (first panel); performances are also translated into a 95% CL upper limit (UL) on $\mathcal{B}(\tau \to e\phi)$ as a function of m_ϕ, with a given Belle-II luminosity $\mathcal{L}$,[1] see the middle and rightmost panels of fig. 3.

Specifically, the middle panel of fig. 3 shows the UL for the different luminosities $\mathcal{L} = \{0.1, 1, 50\}$ ab^{-1}, that roughly correspond to the Summer 2021 dataset, the dataset as of the 2022 shutdown, and the full Belle-II dataset, respectively. On the other hand, the rightmost panel displays a comparison among the cases discussed above, at the fixed luminosity $\mathcal{L} = 0.1$ ab^{-1}. We can synthesize by saying that, for an ALP or hidden vector of small $m_\phi \lesssim 1$ MeV, our full strategy applied to the 1×3 channel alone is expected to provide a 95%-CL limit of around

$$\begin{aligned} \mathcal{B}(\tau \to e\phi) &\leq \{5.4 \cdot 10^{-5}, 1.7 \cdot 10^{-5}, 2.4 \cdot 10^{-6}\}, \\ \text{for } \mathcal{L} &= \{0.1, 1, 50\} \text{ ab}^{-1}. \end{aligned} \tag{7}$$

These figures are to be compared with $\mathcal{B}(\tau \to e\phi) \leq \{1.3 \cdot 10^{-4}, 4.0 \cdot 10^{-5}, 5.7 \cdot 10^{-6}\}$ with the thrust method alone. In conclusion, our strategy sharpens by a factor close to 3 the UL that can be obtained with the state-of-the-art Belle II strategy of [7]. The Belle-II limit on BR($\tau \to e$ + invisible) that follows from our analysis will be stronger than the existing ARGUS limit [6] by a factor of 50, 170, 1150, respectively, with 0.1, 1, 50 ab^{-1} Belle-II data.

I conclude by noting that the above approach has a vast potential of applicability to the extent that the underlying, pairwise decay topology is the same. For example, a similar approach may also be applied to B decays, and in fact one such application is work in progress.

Acknowledgments

I would like to thank the organizers, in particular Gui Rebelo and George Zoupanos, for the kind invitation to this enjoyable workshop.

References

[1] J. Beacham et al., *Physics Beyond Colliders at CERN: Beyond the Standard Model Working Group Report*, *J. Phys.* **G47** (2020) 010501, [1901.09966].

[1] As mentioned before, we obtain such limit through a completely different procedure than in Ref. [7]. Our procedure is described in detail in Ref. [18].

[2] G. Lanfranchi, M. Pospelov and P. Schuster, *The Search for Feebly-Interacting Particles*, 2011.02157.

[3] H. Georgi, D. B. Kaplan and L. Randall, *Manifesting the Invisible Axion at Low-energies*, *Phys. Lett.* **169B** (1986) 73–78.

[4] L. Calibbi, D. Redigolo, R. Ziegler and J. Zupan, *Looking forward to lepton-flavor-violating ALPs*, *JHEP* **09** (2021) 173, [2006.04795].

[5] MARK-III collaboration, R. M. Baltrusaitis et al., *τ Leptonic Branching Ratios and a Search for Goldstone Decay*, *Phys. Rev. Lett.* **55** (1985) 1842.

[6] ARGUS collaboration, H. Albrecht et al., *A Search for lepton flavor violating decays $\tau \to e\alpha$, $\tau \to \mu\alpha$*, *Z. Phys.* **C68** (1995) 25–28.

[7] F. Tenchini, M. Garcia-Hernandez, T. Kraetzschmar, P. K. Rados, E. De La Cruz-Burelo, A. De Yta-Hernandez et al., *First results and prospects for tau LFV decay $\tau \to e + \alpha$(invisible) at Belle II*, *PoS* **ICHEP2020** (2021) 288.

[8] S. Brandt, C. Peyrou, R. Sosnowski and A. Wroblewski, *The Principal axis of jets. An Attempt to analyze high-energy collisions as two-body processes*, *Phys. Lett.* **12** (1964) 57–61.

[9] E. Farhi, *A QCD Test for Jets*, *Phys. Rev. Lett.* **39** (1977) 1587–1588.

[10] C. G. Lester and D. J. Summers, *Measuring masses of semiinvisibly decaying particles pair produced at hadron colliders*, *Phys. Lett.* **B463** (1999) 99–103, [hep-ph/9906349].

[11] A. Barr, C. Lester and P. Stephens, *m(T2): The Truth behind the glamour*, *J. Phys.* **G29** (2003) 2343–2363, [hep-ph/0304226].

[12] A. J. Barr, T. J. Khoo, P. Konar, K. Kong, C. G. Lester, K. T. Matchev et al., *Guide to transverse projections and mass-constraining variables*, *Phys. Rev.* **D84** (2011) 095031, [1105.2977].

[13] W. S. Cho, K. Choi, Y. G. Kim and C. B. Park, *M(T2)-assisted on-shell reconstruction of missing momenta and its application to spin measurement at the LHC*, *Phys. Rev.* **D79** (2009) 031701, [0810.4853].

[14] C. B. Park, *Reconstructing the heavy resonance at hadron colliders*, *Phys. Rev.* **D84** (2011) 096001, [1106.6087].

[15] G. G. Ross and M. Serna, *Mass determination of new states at hadron colliders*, *Phys. Lett.* **B665** (2008) 212–218, [0712.0943].

[16] W. S. Cho, J. S. Gainer, D. Kim, K. T. Matchev, F. Moortgat, L. Pape et al., *On-shell constrained M_2 variables with applications to mass measurements and topology disambiguation*, *JHEP* **08** (2014) 070, [1401.1449].

[17] D. Kim, K. T. Matchev, F. Moortgat and L. Pape, *Testing Invisible Momentum Ansatze in Missing Energy Events at the LHC*, *JHEP* **08** (2017) 102, [1703.06887].

[18] D. Guadagnoli, C. B. Park and F. Tenchini, $\tau \to \ell$ + *invisible through invisible-savvy collider variables*, *Phys. Lett. B* **822** (2021) 136701, [2106.16236].

[19] K. Agashe, D. Kim, D. G. E. Walker and L. Zhu, *Using M_{T2} to Distinguish Dark Matter Stabilization Symmetries*, *Phys. Rev.* **D84** (2011) 055020, [1012.4460].

[20] ILD Design Study Group collaboration, H. Li, K. Ito, R. Poschl, F. Richard, M. Ruan, Y. Takubo et al., *HZ Recoil Mass and Cross Section Analysis in ILD*, 1202.1439.

[21] K. Fujii et al., *Physics Case for the International Linear Collider*, 1506.05992.

[22] K. Hagiwara, T. Li, K. Mawatari and J. Nakamura, *TauDecay: a library to simulate polarized tau decays via FeynRules and MadGraph5*, *Eur. Phys. J.* **C73** (2013) 2489, [1212.6247].

[23] C. B. Park, *YAM2: Yet another library for the M_2 variables using sequential quadratic programming*, *Comput. Phys. Commun.* **264** (2021) 107967, [2007.15537].

[24] A. Hoecker, P. Speckmayer, J. Stelzer, J. Therhaag, E. von Toerne and H. Voss, *TMVA: Toolkit for Multivariate Data Analysis*, *PoS* **ACAT** (2007) 040, [physics/0703039].